



ISSN 0975-413X
CODEN (USA): PCHHAX

Der Pharma Chemica, 2016, 8(1):312-322
(<http://derpharmachemica.com/archive.html>)

Chemical nuclease activity of acenaphthenequinone derived Schiff Base Copper (II) complexes: Design, synthesis, structural elucidation and epr activity

S. Magala Sathyasheeli¹, S. Theodore David*², C. V. Mythili³ and P. S. Suja Pon Mini²

¹Department of Chemistry, Infant Jesus College of Engineering, Keelavallanadu, Thoothukudi, India

²Research Department of Chemistry, PSN College of Engineering and Technology, Tirunelveli, India

³Department of Chemistry, Rani Anna Government College for Women, Tirunelveli, India

ABSTRACT

Three new 'NNOO' type tetradentate Schiff base ligands have been synthesised by the condensation of Acenaphthenequinone with essential amino acids in 1:2 stoichiometry. They were complexed with copper and structurally characterized by analytical techniques like molar conductance, magnetic studies and spectral techniques like ¹³C NMR, EI-Mass, FT-IR, UV-Visible spectra, EPR spectra etc. The complexes are non-electrolytes. The Schiff bases act as tetradentate ligand leading to square planar geometry around Cu (II) in all the three complexes. The electrochemical studies explain the change of structural arrangement of the ligand around Cu (II) ions. The metal complexes are subjected to DNA cleavage with pUC19DNA. The invitro antibacterial assay of the complexes against gram positive and gram negative strains indicate that they are biocidal agents.

Keywords: acenaphthenequinone, aminoacids, DNA Cleavage, antibacterial assay.

INTRODUCTION

Schiff bases, due to their extensive applications play a pivotal role in the development of co-ordination and bio-inorganic chemistry. Acenaphthenequinone based Schiff bases are widely synthesized due to their potential applications in various areas [1-5]. Amino acids constitute the building blocks of proteins and are indispensable for performing large number of biological functions [6-7]. Multiple functional groups (COOH, NH₂) present in the amino acid side chain of the ligands can lead to the development of unexpected and unusual structures [8-9]. The mononuclear and multinuclear metal complexes have great impact in different areas of chemistry like organic, inorganic, bio-inorganic and medicinal chemistry. Here we have reported the synthesis, characterization and DNA cleavage studies of the copper complexes of Acenaphthenequinone with essential amino acids like glycine, cysteine and methionine.

MATERIALS AND METHODS

All the reagents involved in this work were purchased in pure form and used as such. Solvents used are either of 99% purity or purified by known laboratory procedure [10]. Tris HCl buffer, Nutrient medium were purchased from Himedia. pUC 19 DNA was procured from Genie Company, Bangalore.

2.2 Instrumental

The microanalysis of Carbon, Hydrogen and Nitrogen was recorded on Elementer Vario EL III elemental analyser. The mass spectral analysis was carried out in JEOL-300 mass spectrometer. The room temperature FT-IR spectra for the ligand and complexes were recorded as KBr pellets with SHIMADZU FT-IR 8400S spectrometer in the range of

4000-400 cm^{-1} . The molar conductance values for the complexes were measured using Systronic Conductivity bridge type using DMF solvent. The magnetic susceptibility measurement was done on a modified Hertz SG8-5HJ model Guoy magnetic balance. UV-Visible spectra were recorded using perkin Elmer Lambda 35 UV-Visible spectrophotometer in the range of 190-1100 nm using DMF as the solvent. Cyclic Voltammetric studies of the synthesized complexes were carried out at room temperature with Impedance analyzer cum cyclic voltammeter, VersaSTAT MC in DMF solution containing 0.1M NaClO_4 using a glassy carbon electrode. The X-band EPR spectrum of the copper complexes in DMSO was recorded with JEOL model JES FA200 spectrometer at Liquid Nitrogen temperature (LNT).

2.3 Synthesis of Schiff base ligand and its metal complexes

Synthesis of Schiff base ligand

2 mmol of Acenaphthenequinone (A) and 4 mmol of the amino acid (L-Glycine(B)/L-Cysteine(D)/L-Methionine(E)) were dissolved in 40 ml of warm Dichloromethane. The reaction mixture was stirred overnight on a magnetic stirrer to give yellow coloured precipitate. The precipitate was washed with water and then with diethylether. It was then dried in vacuum.

Synthesis of Schiff base metal complexes

An equimolar (1mmol) methanolic solution of the Schiff base ligand (AB/AD/AE) and copper(II)chloride dihydrate were stirred and refluxed at 50°C for 8 hours. The precipitated metal complexes were filtered, washed with ethanol, ether and dried in vacuum.

2.4 DNA Cleavage

The DNA Cleavage studies of the synthesized molecules were carried out by agarose gel electrophoresis method [11]. The gel electrophoresis experiments were performed by the incubation of the samples containing 40 μm pUC DNA, 50 μm metal complexes and 50 μm H_2O_2 in Tris-HCl buffer (7.7) at 37°C for 2 hours. After incubation, the samples were subjected to electrophoresis for 2 hours at 50V on 1% agarose gel using Tris-acetic acid-EDTA buffer. The gel was then stained using 1 $\mu\text{g cm}^{-3}$ ethidium bromide (EB) and photographed under ultra violet light at 360nm [12].

2.5 Antimicrobial Studies

The invitro antibacterial efficiency of the complexes was tested against *Bacillus subtilis*, *Staphylococcus aureus*, *Escherichia coli*, *Klebsiella pneumonia* and *Pseudomonas aeruginosa* by agarwell diffusion method. Muller-Hinton agar (MHA) plates were swabbed with overnight culture of respective bacteria. Wells were made in each of these plates using sterile cork borer. Required amount of the solution of metal complexes were added into the wells and allowed to diffuse at room temperature for 2hrs. Control experiments comprising inoculums with cefatoxime disc were set up. The plates were incubated at 37°C for 18-24 h. The diameter of the inhibition zone (mm) was measured and the activity was calculated.

RESULTS AND DISCUSSION

All the synthesized complexes are found to be stable in air and non-hygroscopic in nature. The complexes are insoluble in common organic solvents but are soluble in DMSO and DMF.

3.1 Elemental Analysis and Molar conductance

Schiff base ligands are formed by the condensation of 1 mmol of acenaphthenequinone (A) with 2mmol of amino acids, viz. L-Glycine(B)/L-Cysteine(D)/L-Methionine(E). The elemental analysis data agree with the calculated values. The observed molar conductance value of the complexes in DMF supports the non-electrolytic nature of the complexes which further suggests the absence of counter ion in the proposed structure (Fig.1). The analytical data of the complexes are given in Table 1.

Table1. Analytical Data of the Schiff base complexes

Compound	Empirical Formula	Yield (%)	% of elements, Found (Calc)				Molar conductance	Magnetic moment (BM)
			C	H	N	Cu		
CuAB	$\text{C}_{16}\text{H}_{10}\text{N}_2\text{O}_4\cdot\text{Cu}$	61	53.7 (53.9)	2.8 (2.9)	7.8 (7.8)	17.63 (17.78)	16.10	1.76
CuAD	$\text{C}_{18}\text{H}_{14}\text{N}_2\text{O}_4\text{S}_2\cdot\text{Cu}$	58	47.80 (48.05)	3.02 (3.11)	6.11 (6.23)	14.06 (14.13)	26.3	1.83
CuAE	$\text{C}_{22}\text{H}_{20}\text{N}_2\text{O}_4\text{S}_2\cdot\text{Cu}$	53	52.38 (52.43)	3.91 (3.97)	5.48 (5.56)	12.59 (12.62)	24.1	1.84

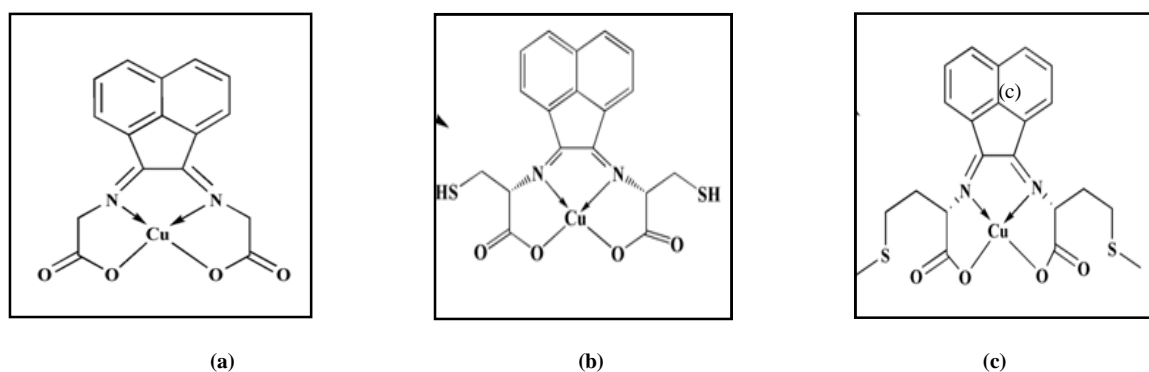
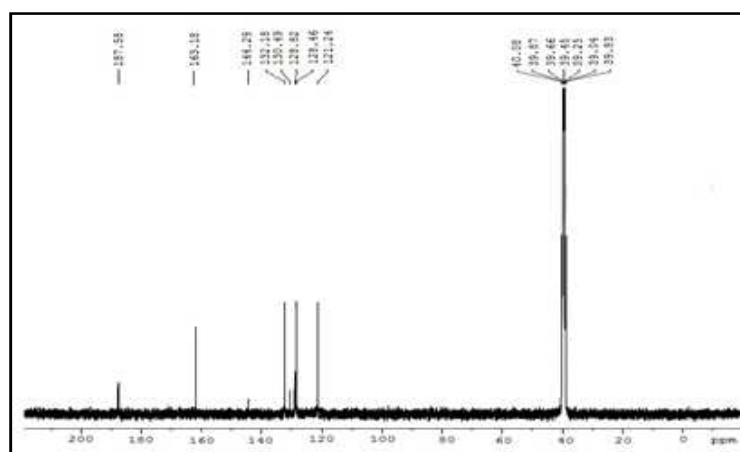


Fig.1. Structure of (a) CuAB (b) CuAD (c) CuAE

3.2 ^{13}C NMR Spectral Studies

The ^{13}C NMR spectrum of the Schiff base ligand AB, AD and AE recorded in CDCl_3 is given in Fig.2, S1, S2. It exhibits 4 signals confirming the presence of 4 different types of carbon atoms. The set of signals at 122.24 to 144.29 ppm is assigned to aromatic carbon atoms, Carboxylic carbon is observed at 187.5 ppm and the signal at 163.18 ppm confirms the presence of azomethine carbon, thus authenticating the formation of Schiff base.

Fig.2. ^{13}C NMR spectrum of the Schiff base ligand AB, recorded in CDCl_3

3.3 Fourier Transform-Infrared (FT-IR) spectra

The vibrational spectra of Schiff base AB, AD and AE represented in Figures 3, S₃ and S₄ confirms the formation of imine peak observed at 1597cm^{-1} , 1596cm^{-1} and 1596cm^{-1} respectively [13]. During complexation, the imine peak is shifted to 1590cm^{-1} , 1585cm^{-1} and 1578cm^{-1} respectively (Figures 4, S₅ and S₆). This indicates the co-ordination of free ligand with copper through imino nitrogen. Furthermore, the asymmetric stretching frequency due to COO^- in the free ligands occurring around 1720cm^{-1} , 1722cm^{-1} has been shifted around 1705cm^{-1} , 1683cm^{-1} and the symmetrical stretching band at 1432cm^{-1} and 1485cm^{-1} is shifted to lower wavelength region confirming the coordination of Cu(II) ion with carboxylato oxygen group. This is further assured by the presence of a band at 515cm^{-1} , 531cm^{-1} characteristic of M–N bond of the complexes. This is also confirmed by the appearance of the peak at 414cm^{-1} and 428cm^{-1} corresponding to M–O bond. The IR spectral data containing the relevant vibrational bands of copper (II) complexes are listed in Table 2.

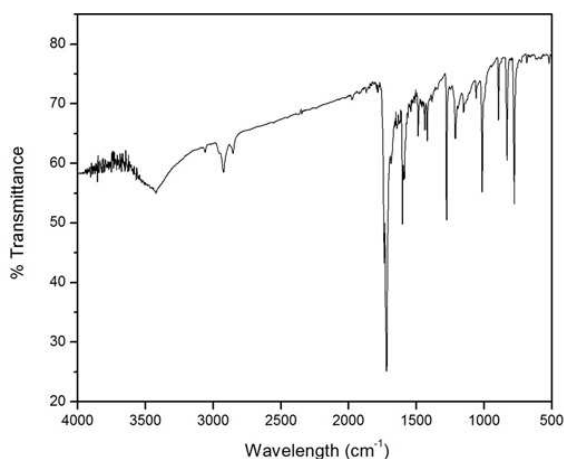


Fig.3. Vibrational Spectrum of Schiff base (AB)

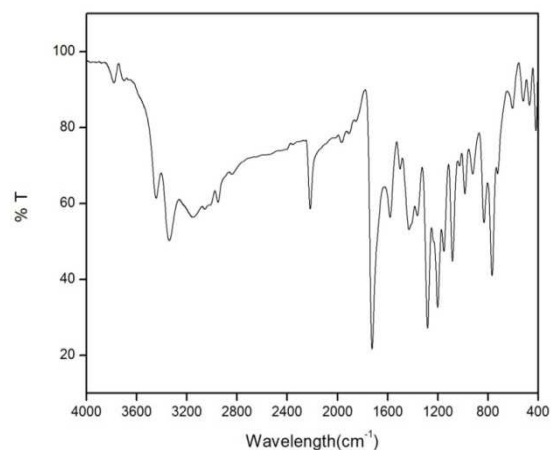


Fig.4. Vibrational Spectrum of CuAB

Table.2. IR Spectral data of Schiff base and its copper complexes

Compound	$\nu(\text{C}=\text{N})$	$\nu(\text{COO})_s$	$\nu(\text{COO})_{as}$	$\nu(\text{M}-\text{O})$	$\nu(\text{M}-\text{N})$
AB	1597	1720	1432	---	---
AD	1596	1722	1484	---	---
AE	1596	1720	1485	---	---
CuAB	1590	1706	1419	428	531
CuAD	1585	1683	1404	414	515
CuAE	1578	1705	1432	416	515

3.4 Electronic Spectroscopy

Electronic spectrum is used to deduce the nature of ligand field around the metal ion. The electronic spectrum of all copper complexes displayed in Figures 5a, 5b, S₇ and S₈ exhibits two characteristic absorption bands at 671 nm and 512 nm for CuAB, 649 nm and 503 nm for CuAD, 676 nm and 505 nm for CuAE corresponding to ${}^2\text{B}_{1g}$, ${}^2\text{E}_g$ and ${}^2\text{B}_{1g}$, ${}^2\text{A}_{1g}$ transitions [14]. Hence, dsp^2 hybridised square planar geometry can be assigned to all Cu (II) complexes. It is further confirmed by EPR spectra.

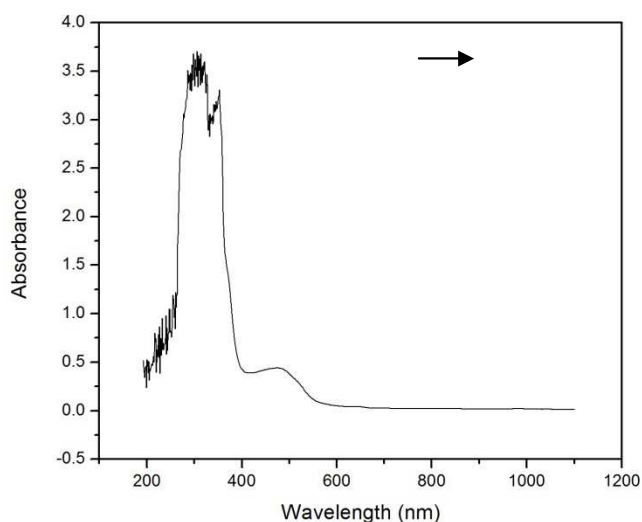


Fig. 5a. Electronic spectrum of CuAB complex (200-1200nm)

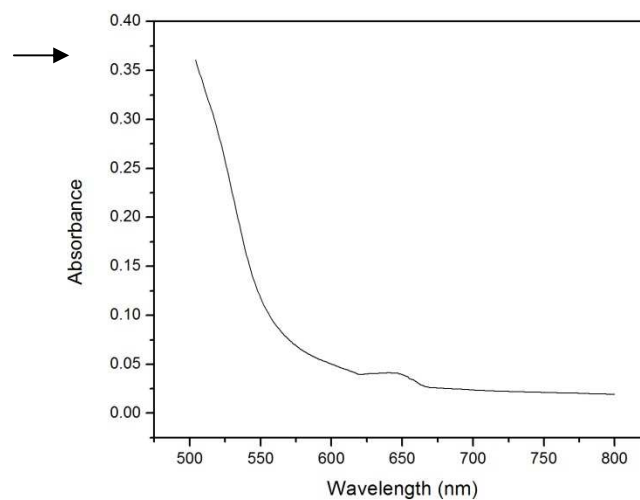


Fig. 5b. Electronic spectrum of CuAB complex (500-800nm)

3.5 Cyclic Voltammetry

Electrochemical behavior depends on the structure and size of the substituent. The cyclic voltammogram of CuAB complex in Fig.6 exhibits well defined waves in cathodic and anodic regions. A wave corresponding to the reduction of Cu(II) to Cu(I) was obtained at the potential, $E_{p_c} = -0.71\text{V}$. During the reverse scan, the oxidation of Cu(I) to Cu(II) occurred at the potential $E_{p_a} = -1.2\text{V}$. The value of limiting peak to peak separation ($\Delta E_p = -0.61\text{V}$) revealed that this process is quasi reversible [15]. An irreversible anodic peak obtained at $E_{p_a} = 1.2\text{V}$ corresponds to ligand

oxidation. The Cyclic voltammogram of CuAD complex depicted in Fig.S₉ shows a quasi reversible cathodic peak at $E_{p_c} = -0.5V$ with corresponding anodic peak at $E_{p_a} = -1.25V$ is assigned to the formation of Cu(II) /Cu(I) couple. The cyclic voltammogram of CuAE complex is represented in Fig.S₁₀. The redox cathodic peak appearing at $E_{p_c} = -0.75V$, $E_{p_a} = -1.25V$ indicates the reaction of the complex on the glassy carbon electrode surface is quasi reversible redox process assigned to the formation of Cu(II) / Cu(I) couple.

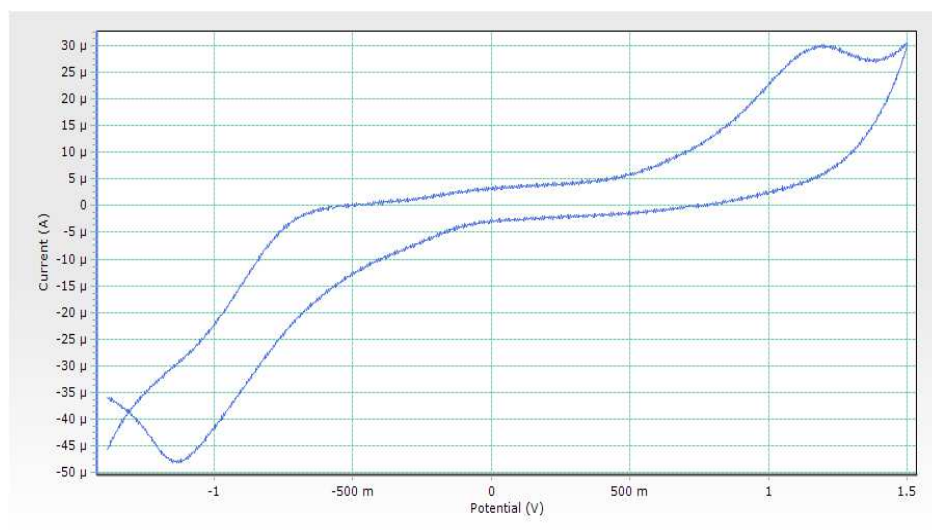


Fig.6. Cyclic Voltammogram of CuAB complex

3.6 Electron Spin Resonance Spectral Studies

The ESR spectrum provides information about the sharing of unpaired electron and the nature of bonding between metal ions and ligands. The ESR spectrum of all the complexes was recorded at Liquid Nitrogen Temperature in DMSO solution in X-band and is given in Figures 7, S₁₁ and S₁₂. The g tensor value was calculated relative to the standard marker DPPH ($g = 2.0023$). From the observed value, $g_{\parallel} = 2.23$, $g_{\perp} = 2.027$ for CuAB, $g_{\parallel} = 2.22$, $g_{\perp} = 2.040$ for CuAD, $g_{\parallel} = 2.041$, $g_{\perp} = 2.0086$ for CuAE it is clear that $g_{\parallel} > g_{\perp} > 2.0023$ hence confirming square planar geometry for copper complexes. This is also supported by the fact that the unpaired electron lies predominantly in $d_{x^2-y^2}$ orbital [16, 17].

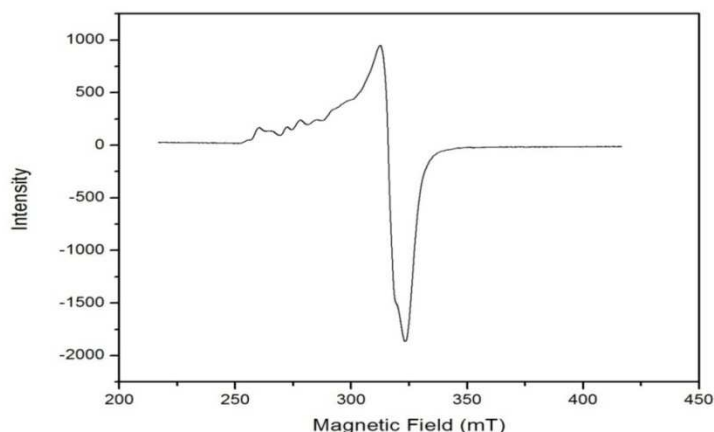


Fig.7. ESR spectrum of the CuAB complex at LNT

3.7 Chemical Nuclease Activity

The DNA cleavage activities of Cu (II) complexes have been studied by gel electrophoresis and a representative pictograph is shown in Fig.8. The results showed that the supercoiled pUC 19 DNA in buffer medium (pH=7.2; Tris-HCl) was converted into open circular form (Form II) and finally to Linear form (Form III). The completion of gel electrophoresis experiment clearly indicates that the intensity of the treated DNA samples has diminished due to the cleavage of DNA. This concludes that all copper complexes except CuAB cleave DNA compared to control DNA in the presence of H_2O_2 and most cleavage cases are caused by copper ions reacting with H_2O_2 to produce diffusible hydroxyl radical ($-OH$) or molecular oxygen, which may damage the DNA through Fenton type chemistry [18,7]

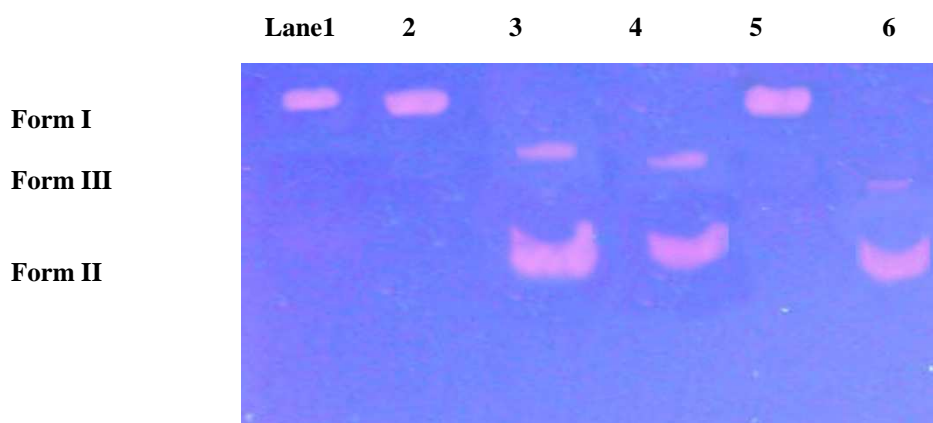


Fig.8. Gel electrophoresis diagram showing the cleavage of pUC 19 DNA by the synthesized complexes in the presence of H_2O_2 . lane 1, DNA control; lane 2, DNA + CuAC; lane 3, DNA + CuAC + H_2O_2 ; lane 4, DNA + CuAD + H_2O_2 ; lane 5, DNA + CuAB + H_2O_2 and lane 6, DNA + CuAE + H_2O_2

3.8 Antimicrobial Screening

The invitro antimicrobial activity of the synthesized metal complexes on selected gram negative bacterial strains like *Escherichia coli*, *Klebsiella pneumonia*, *Pseudomonas aeruginosa* and gram positive bacterial strains like *Bacillus subtilis*, *Staphylococcus aureus* by agar well diffusion method and is displayed in Fig.9. All the complexes are active towards *Bacillus subtilis* and *Staphylococcus aureus*. CuAB complex shows no activity towards *Klebsiella pneumonia* and CuAE is passive towards *Pseudomonas aeruginosa*. CuAD is least active towards the pathogens. The antimicrobial efficacy of the metal complexes is due to co-ordination and chelation [19,20]. As a result of chelation, the polarity of the central metal atom is reduced, because of the partial sharing of its positive charge with the ligand.

Table.3. Antimicrobial screening of copper complexes by agar well diffusion method (zone formation in mm)

Compound	<i>Bacillus subtilis</i>	<i>Escherichia coli</i>	<i>Klebsiella pneumonia</i>	<i>Pseudomonas aeruginosa</i>	<i>Staphylococcus aureus</i>
CuAB	14	11	-----	15	18
CuAD	12	-----	-----	-----	16
CuAE	16	15	16	-----	14
Control	29	23	30	21	30

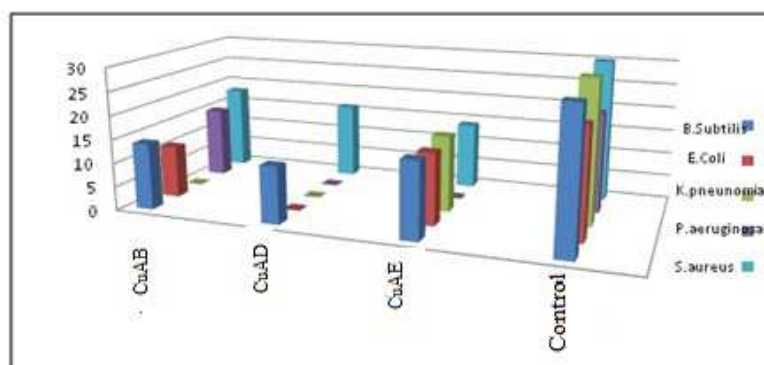


Fig.9. Antimicrobial screening of copper complexes by agar well diffusion method

CONCLUSION

Three novel Schiff base ligands (AB, AD, AE), their copper complexes have been synthesized and their structure, morphology, physical and chemical properties are determined by IR, UV-Visible, ^{13}C and mass spectral studies. The Schiff base ligands bind the metal ions in a tetradentate mode through two azomethine nitrogen and two carboxylato oxygen atoms. Spectral studies suggest square planar geometry and EPR studies confirm the square planar geometry for the complexes. The results of chemical nuclease activity performed by agarose gel electrophoresis using supercoiled pUC19 DNA reveals that CuAD and CuAE complexes cleave the DNA efficiently from supercoiled form to linear form. The invitro antibacterial activity of the synthesized complexes shows potent antibacterial activity against *B.subtilis* and *S.aureus* species.

REFERENCES

- [1] R B Xu, N Zhang, H Y Zhou, S P Yang, Y Y Li, D H Shi, W X Ma, X Y Xu, *Journal of Chemical Crystallography*, **2012**, 42, 928-932.
- [2] L G Wade, "Organic Chemistry", 6th Edition, Pearson Prentice Hall, Upper Saddle river, 2005.
- [3] R J Mandanis, J S Wood, A Chandrasekaran, M D Rausch, J C W Chien, *Journal of Organometallic Chemistry*, **2002**, 645, 158-167.
- [4] I Mhaidat, J A Mergos, S Kamilakis, C Kollia, Z Loizos, A Tsolomitis, C T Dervos, *Materials Letters*, **2009**, 63, 2587-2590.
- [5] Y G Li, L Pan, Z J Zheng, Y S Li, *Journal of Molecular Catalysis A: Chemical*, **2008**, 287 57-64.
- [6] K H Zimmermann, An introduction to Protein Informatics, Kluwer Academic Publishers, London, 2003.
- [7] M A Neelakantan, R Rusalraj, J Dharmaraja, S Johnsonraja, T Jeyakumar, M S Pillai, *Spectrochim Acta A*, **2008**, 71, 1599-1609.
- [8] Z H Chohan, M Arif, M Sarfraz, *Appl.Organomet.chem*, **2007**, 21, 294-302.
- [9] B K Singh, H Rajour, A Prakash, *Spectrochim Acta A*, **2012**, 94, 143-151.
- [10] D D Perrin, W L F Armarego, D R Perrin, Purification of Laboratory Chemicals, Pergamon Press, New York, 1980.
- [11] N Raman, R.Jeyamurugan, A.Sakthivel, L.Mitu, *Spectrochim.Acta A.*, **2010**, 75, 88-97.
- [12] Pragathi Jogi, Padmaja M, K V T S Pavankumar, Gyanakumari, *J.Chem.Pharm.Res*, **2010**, 4(2), 1389-1397.
- [13] K M El-Shaieh, *Journal of the Chinese Chemical Society*, **2008**, 55, 1150-1155.
- [14] H Unver, Z Hayavali, *Spectrochim.Acta A* **2010**, 75, 782-788.
- [15] N Raman, A Selvan, S Sudharsan, *Spectrochim. Acta A* **2011**, 79, 873-883.
- [16] Ray R K, Kauffman G B *Inorg.Chem.Acta* **1990**, 173, 207.
- [17] Jeyasubramanian K, Samath S A, Thambidurai S, Murugesan R, Ramalingam S K *Trans.Met.Chem.* **1996**, 20, 76.
- [18] A Y Louie, T J Meade, *Chem.Rev.* **1999**, 99, 2711.
- [19] Z H Chohan, M Arif, M A Akhtar, C T Supuran, *Bio inorg.chem.Appl.*, **2006 (2006)** 1-13.
- [20] Z. H. Chohan, A. Scozzafava, C. T. Supuran, *J. Enzyme Inhib.Med.Chem.*, **18 (2003)** 259-263.

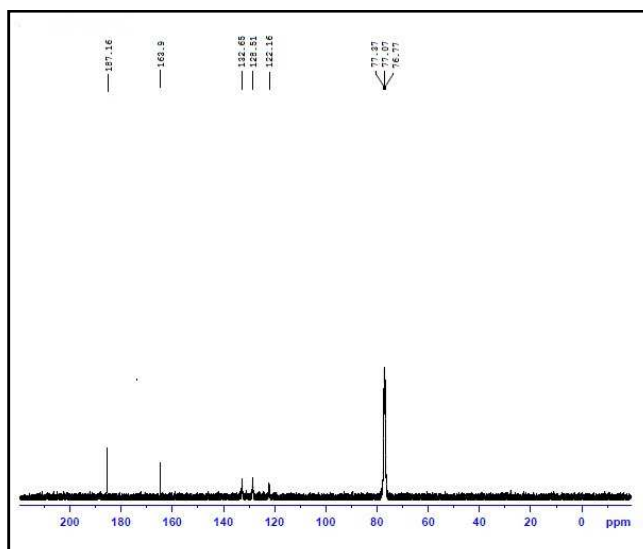


Fig.S1. ^{13}C NMR spectrum of the Schiff base ligand AD, recorded in CDCl_3

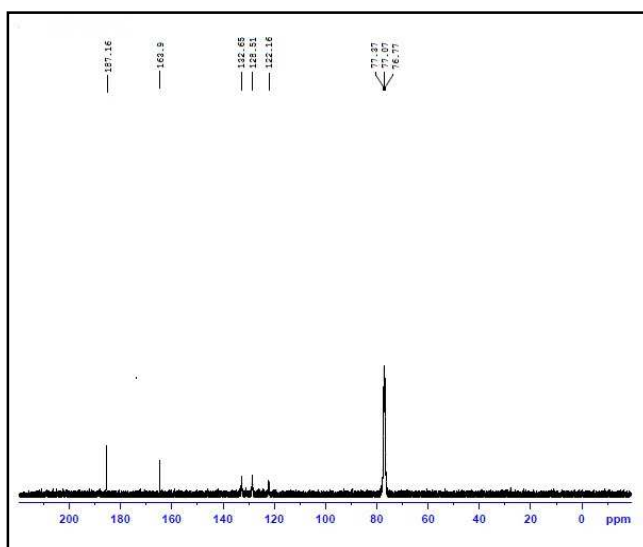


Fig.S2. ^{13}C NMR spectrum of the Schiff base ligand AE, recorded in CDCl_3

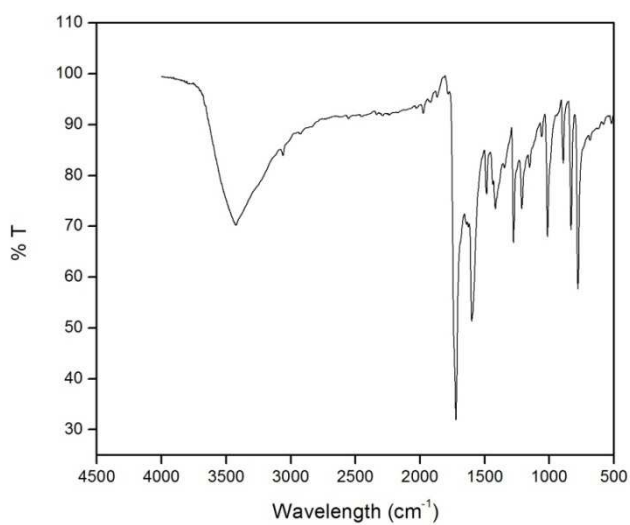
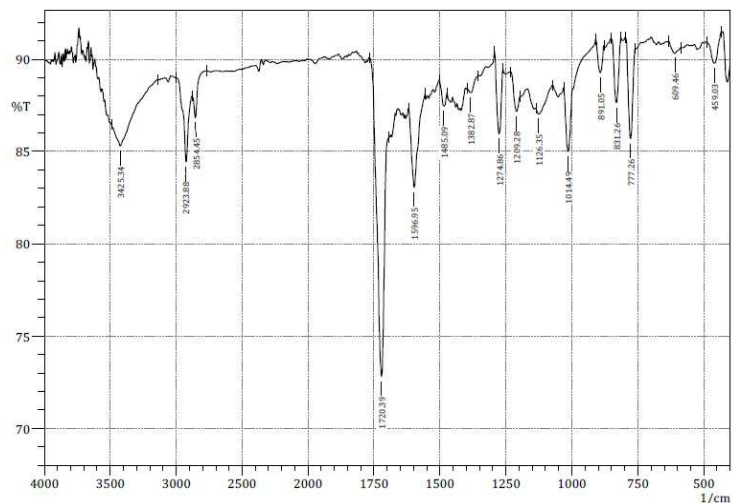
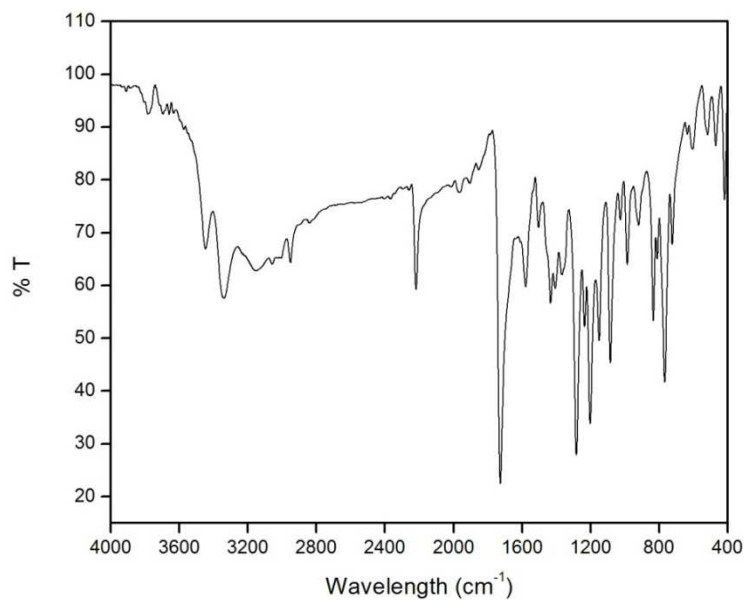
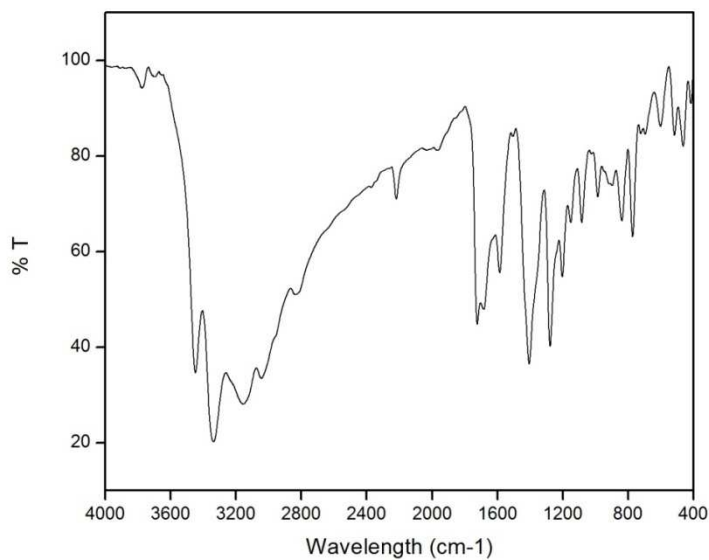


Fig.S3. Vibrational Spectrum of Schiff base ligand(AD)

**Fig.S4. Vibrational Spectrum of Schiff base ligand(AE)****Fig.S5. Vibrational Spectrum of CuAD complex****Fig.S6. Vibrational Spectrum of CuAE complex**

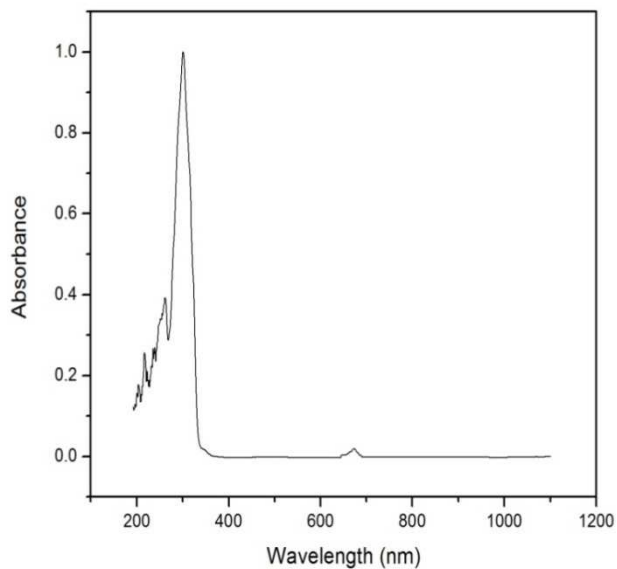


Fig.S7a. Electronic spectrum of CuAD

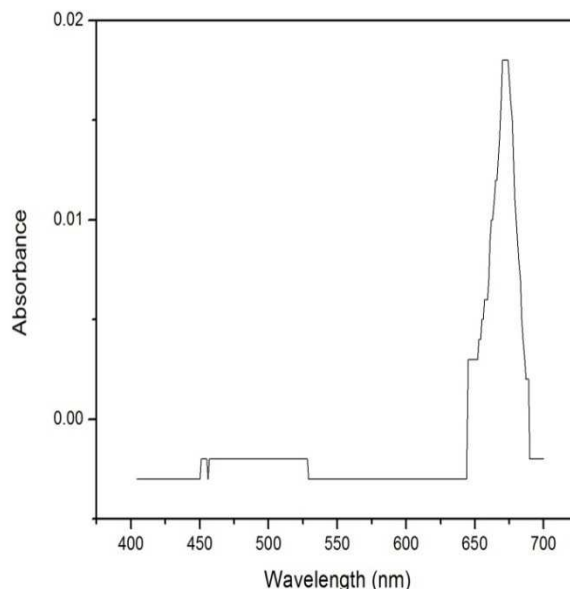


Fig.S7b. Electronic spectrum of CuAD

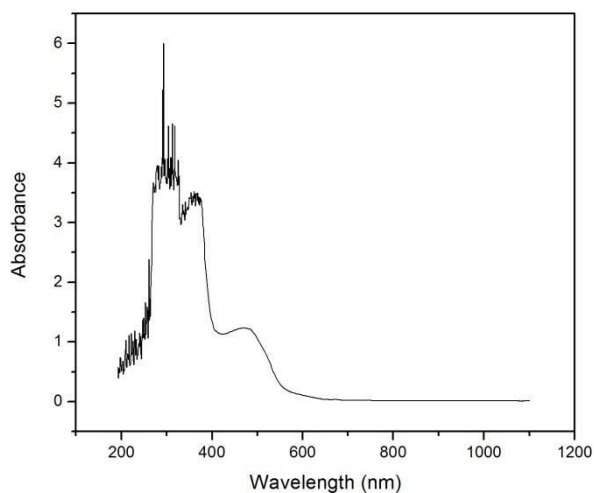


Fig.S8a. Electronic spectrum of CuAE

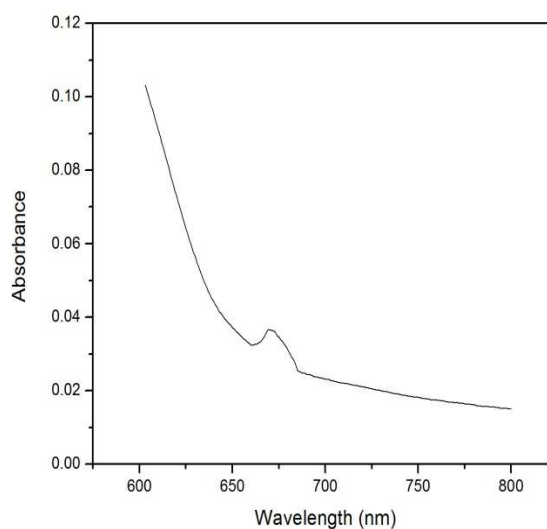


Fig.S8b. Electronic spectrum of CuAE

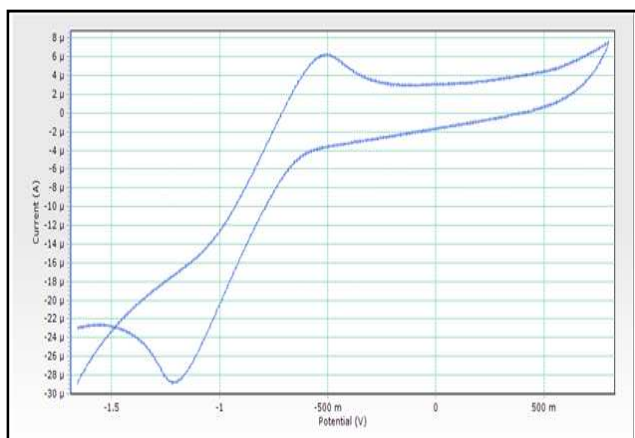


Fig.S9. Cyclic Voltammogram of CuAD complex

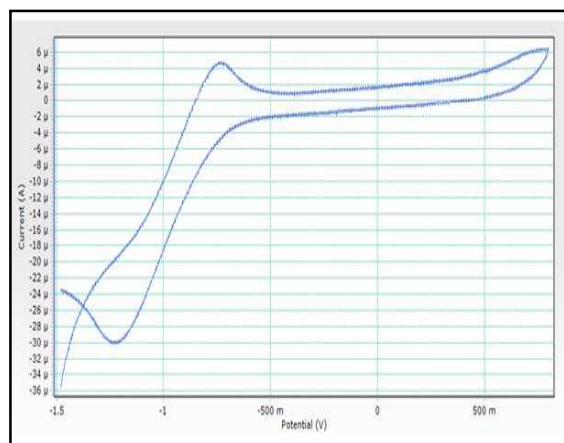


Fig.S10. Cyclic Voltammogram of CuAE complex

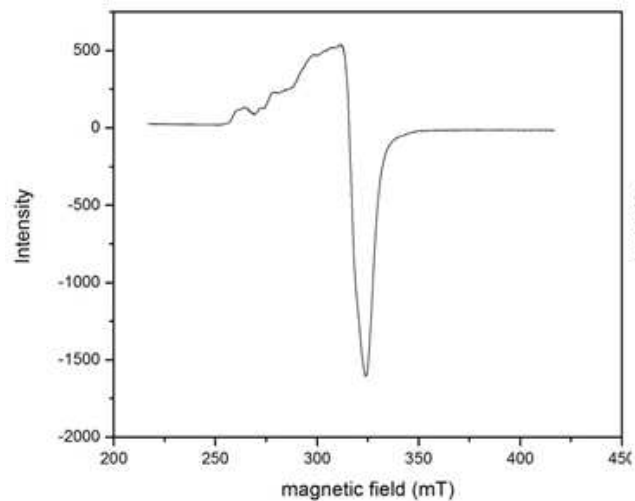


Fig.S11. ESR spectrum of the CuAD complex at LNT

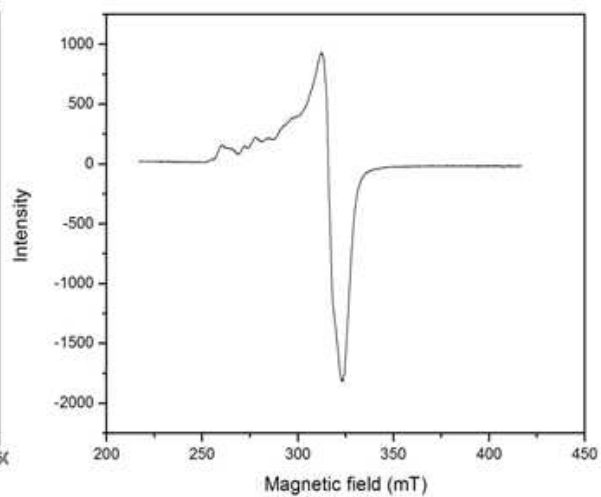


Fig.S12. ESR spectrum of the CuAE complex at LNT